Alexandria Engineering Journal (2016) 55, 2539–2550

HOSTED BY

Alexandria University

Alexandria Engineering Journal

www.elsevier.com/locate/aej
www.sciencedirect.com

ORIGINAL ARTICLE

Adaptive protection scheme for smart microgrid with electronically coupled distributed generations

R. Sitharthan [a,*], M. Geethanjali [b], T. Karpaga Senthil Pandy [b]

[a] MVJ College of Engineering, Bangalore 560 067, India
[b] Thiagarajar College of Engineering, Tamil Nadu 625015, India

Received 18 April 2016; accepted 27 June 2016
Available online 8 August 2016

KEYWORDS

Distributed power generation;
Microgrids;
Power system protection;
Power generation control;
Wind energy generation;
PEM fuel cell

Abstract This paper aims at modelling an electronically coupled distributed energy resource with an adaptive protection scheme. The electronically coupled distributed energy resource is a microgrid framework formed by coupling the renewable energy source electronically. Further, the proposed adaptive protection scheme provides a suitable protection to the microgrid for various fault conditions irrespective of the operating mode of the microgrid: namely, grid connected mode and islanded mode. The outstanding aspect of the developed adaptive protection scheme is that it monitors the microgrid and instantly updates relay fault current according to the variations that occur in the system. The proposed adaptive protection scheme also employs auto reclosures, through which the proposed adaptive protection scheme recovers faster from the fault and thereby increases the consistency of the microgrid. The effectiveness of the proposed adaptive protection is studied through the time domain simulations carried out in the PSCAD\EMTDC software environment.

1. Introduction

Energy crisis is one of the most important and crucial problems faced by the world in the present decades. Conventional resources that are used for energy production cause environmental pollution and their severe consequences affect the humans in their day-to-day life. To tackle this problem, the energy sector has started to generate its energy requirement through the Renewable Energy Sources (RES) rather than the conventional fossil fuel based energy generation. This type of RES is commonly called as Distributed Generation (DG) or Dispersed Generation [1]. The combination of DGs and local loads with or without the support from the utility grid is called as "Microgrid" [2]. The formation of microgrid reduces the overall operational burden of the utility grid.

Consequently, the generation of bulk power is possible through microgrid, i.e., multiple modules of independent sources rather than a single concentrated power plant. The DG systems are coupled to microgrid by means of electronic devices to form an Electronically Coupled Distributed Energy Resources (EC-DERs) [3].

The microgrid performs independently to maintain overall reliability and stability of the grid [4]. Furthermore, the behaviour of the microgrid is so dynamic, because coupling and shedding of distributed generators or load may take place at any time in the microgrid [5]. On every occasion of such changes, microgrid behaves erroneously such as generating

* Corresponding author.
E-mail address: sithukky@gmail.com (R. Sitharthan).
Peer review under responsibility of Faculty of Engineering, Alexandria University.

http://dx.doi.org/10.1016/j.aej.2016.06.025

power, sharing the load, and providing protection and control strategies [6]. In order to operate normally, microgrid should adapt to the network parameters [7,8]. Moreover, to solve such situation, the microgrid requires an intelligent administrative system for the entire network to give order for the relay in all branches of the network [9,10]. Consequently, an innovative protection system is required for secured operation of the microgrid [11]. In this regard, several approaches have been discussed for the protective scheme of EC-DER. In an approach, over-current based protection strategy is implemented for rotational Electronically Coupled Distributed Generation (EC-DG) in microgrid [12–14]. This system does not require modified protections relays and hence, is more economical. But, it provides ineffective protection for islanded mode of operation. In another approach, symmetrical component based over-current relay has been developed exclusively for the EC-DG based microgrid operation in islanded mode [15,16]. It provides an excellent response to three phase faults. But, frequent single phase tripping occurs in the system. Later, differential current based protection strategy has been developed for protecting EC-DG connected microgrid [17–19]. This protection strategy can operate in both grid connected mode and islanded mode. Further, this protection system can detect the low impedance fault. But, this protection system does not operate effectively when the microgrid is connected with unbalanced loads [20]. To overcome the existing problems a new approach has been proposed by making modification in the protection scheme.

This paper proposes an adaptive protection scheme for microgrids. The proposed protective scheme uses microprocessor-based over current relays. Furthermore, the significant character of the protection scheme is that it acts independently during the magnitudes of fault current and can act in the both grid connected mode and islanded mode. It also increases the reliability of the microgrid by enabling auto reclosure for temporary faults. Also, the proposed system can detect low impedance fault and it is designed in such a way that the power can flow from source to load in a single direction. Hence, this proposed low cost and simple protection schemes can be utilized for enhancing the power system protection. The effectiveness of the proposed adaptive protection is demonstrated through the simulation study carried out in the PSCAD\EMTDC software environment and the results obtained are compared with the conventional protection scheme. The proposed protection scheme provides adequate protection to the microgrid during grid connected mode and islanded mode of operations, and also improves the reliability of the microgrid.

The paper is organized as follows: Development of electronically coupled distributed generation based microgrid is discussed in Section 2. The development of the proposed protection strategy is prescribed in Section 3. The developments of the proposed adaptive protection relay and the test system are given in Section 4. The results and comparative analysis are given in Section 5.

2. Development of EC-DER based microgrid

The scope of this paper was to establish the adaptive protective scheme for EC-DGR based microgrid. Hence, the Electronic Coupling (EC) is modelled using power electronic converters followed by the renewable energy resources such as wind, solar, fuel cell and battery energy storage as shown in Fig. 1. The EC pumps the power generated by the DG into the microgrid with the help of power electronic converters.

2.1. Modelling the inverter systems

The control strategy for the inverters in the microgrid is selected based on the mode of operation. Both these modes require different functions to be performed by the control strategy. In grid connected mode, the main function to be performed by the inverter is to control the real and reactive power flow. In the islanded mode of operation, microgrid voltage and frequency regulation are the main functions to be performed. The simplified control scheme is shown in Fig. 2. The control scheme in the grid connected mode is commonly called as the current-control mode. In this mode the real and reactive power of the EC-DG is controlled. First, the control scheme directly controls Voltage Source Converter (VSC) output current, which in turn is used to control the real and reactive power by varying the phase angle and the magnitude of the current with respect to the VSC terminal voltage [21]. The unique feature of this control mode is that it automatically acquires the overload protection, since the current regulation is employed in this strategy.

Initially, the voltage and current in each phase are measured using the CT and PT. By means of *abc* to *dq*0 transformation and PLL block, the measured I_{abc} and V_{abc} are converted to give $I_d - I_q$ component. Out of two components, the *d*-axis component is used to control the real power and the *q*-axis component is used to control the reactive power. The obtained *d*–*q* axis current component is compared with the desired set point value of the reference current vector determined from the extractor block using the measured real and reactive power. The obtained error value is given as input to the PI based current controller. The current controller processes the error value and gives reference voltage vectors in *d*–*q* orientation frame. This voltage vectors in *d*–*q* are given as input to the voltage controller. The obtained *d*–*q* references are transformed into stationary reference frame using *dq*0 to *abc* transformation. Therefore, the obtained stationary reference frame is used by the Space Vector Pulse Width Modulation (SVPWM) to generate switching signals for grid coupling VSC [22]. Further, additional RLC filter is used in between converter and transformer for filtering purpose, where $R = 0.0005\ \Omega$, $L = 0.5$ mH and $C = 100\ \mu$F. In the Islanded mode of operation, in addition to the real and reactive power control, the voltage and frequency regulation are also taken into consideration for controlling the inverter. In grid connected mode the need for voltage and frequency regulation is not much emphasized because the host utility grid supports voltage and frequency regulation of the microgrid. The voltage and frequency regulation can be accomplished by encoding the significance of the change in the voltage and frequency in the *d*–*q* reference current vector. The rated voltage and frequency are kept as set point values and then compared with the current value of the EC-DGs. The obtained error signal in *d*–*q* reference frame is passed through a PI controller with suitable gains. The frequency component and voltage component are added to the real and reactive power components respectively, which have already been generated in the reference current block. Hence, the rest of the operation is the same as that like

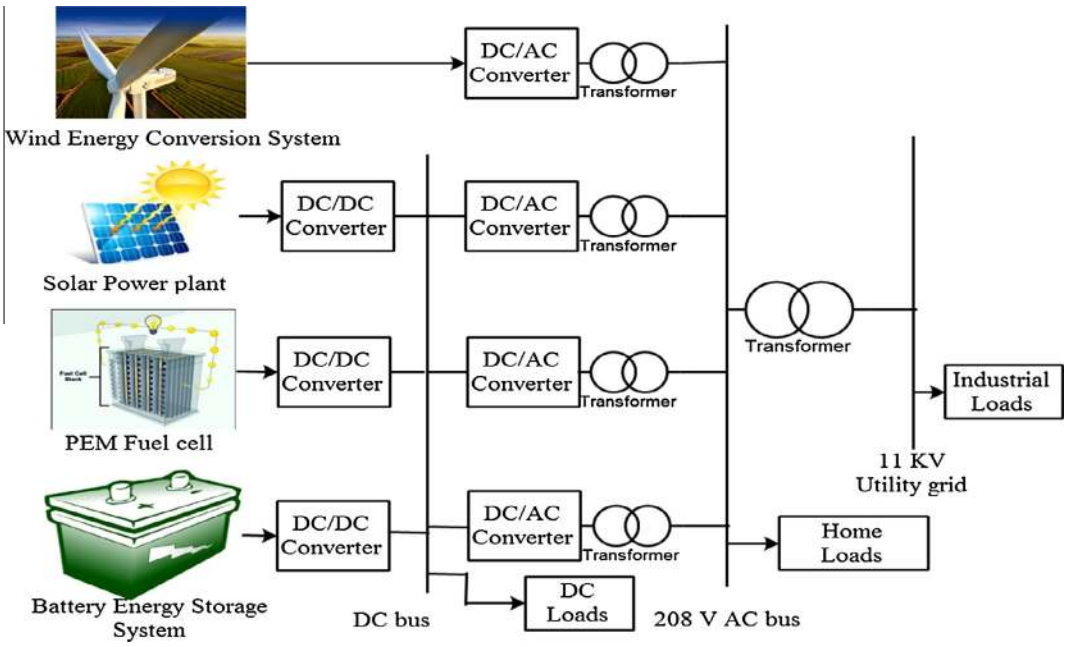

Figure 1 DG system configuration.

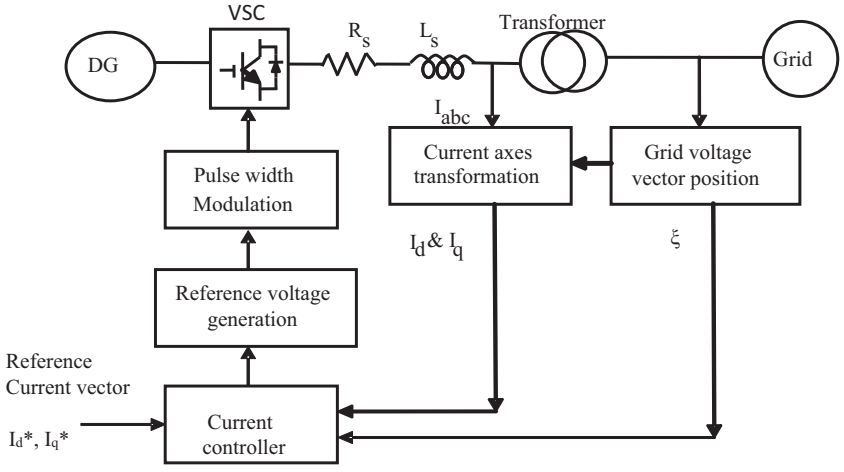

Figure 2 Simplified control scheme of inverter systems.

the grid connected mode. Converters with similar control strategy are used widely to couple the DG to the microgrid.

2.2. Modelling of wind energy conversion system

Doubly fed induction generator based grid coupled wind energy conversion system is developed using PSCAD\EMTDC software environment. This coupling of wind energy conversion system in the microgrid is performed through an AC/DC/AC power electronic converter followed by a step-up transformer [23]. The rated power of the turbine is 1 MVA. The theoretical power available in the wind is given by [24],

$$P_m = 0.5 \times \rho \times C_p \times S \times W_s^3 \tag{1}$$

where P_m – power from the wind turbine, ρ – air density (1.22 kg/m^3), W_s – wind speed (m/s), S – rotor surface (m^2), C_p – wind turbine power co-efficient. Further, the mechanical power from wind turbine is fed to doubly fed induction generator to generate electrical power and is coupled to the microgrid through the modelled power electronic converter.

$$C_p = P_{real}/P_m \tag{2}$$

$$C_p = 1/2(1 - a^2)(1 + a) \tag{3}$$

where α = wind speed behind the rotor/wind speed in front of the rotor. In the standard model of wind turbine defined in the PSCAD master library, the power coefficient is defined using (2)–(4).

$$C_p = 0.5(\gamma - 0.022\beta^2 - 5.6)e^{-0.17\gamma} \tag{4}$$

where $\gamma = 2.237^{*}$ wind speed/hub speed, and β is the incidence angle of the blade. The C_p is calculated for the rated conditions with $\beta = 0$ using Eq. (4). The wind input is applied to the wind turbine whose output is mechanical torque. The mechanical torque from the wind turbine is given as the input to the induction machine; thereby a complete model of the turbine generator is achieved. The output of the induction generator is fed to the rectifier which converts into dc voltage. To maintain the dc-link voltage a capacitor is connected in shunt to the rectifier output. The capacitor is sized to supply energy to the grid up to 1 s when there is a dip in the wind generator output [25]. The dc-link voltage is inverted using the VSC and coupled to the microgrid using a step-up transformer.

2.3. Modelling of solar energy system

A solar cell can be modelled as an electrical equivalent circuit that contains a current source connected with an anti-parallel diode, a shunt resistance and a series resistance. The current I_{SC} is generated when the solar cell is exposed to sunlight. Magnitude of I_{SC} varies linearly with variation in solar irradiance. The current I_D through the anti-parallel diode is major contributor for producing the nonlinear $I-V$ characteristics of the PV cell [26]. The fundamental equation that characterizes the $I-V$ characteristics of a solar cell is given,

$$I = I_{sc} - I_D - I_{sh} \tag{5}$$

$$I_{sc} = I_{scR}\frac{G}{G_R}[1 + \alpha_T(T_c - T_{cR})] \tag{6}$$

$$I = I_{sc} - I_c e^{\left(\frac{V+IR_{sr}}{\frac{nKT_c}{q}}\right)-1-\left(\frac{V+IR_{sr}}{R_{sh}}\right)} \tag{7}$$

$$I_c = I_{cR}\left(\frac{T_c^S}{T_{cR}^S}\right)e^{\left(\frac{1}{T_{cR}}-\frac{1}{T_c}\right)\frac{q_{es}}{nk}} \tag{8}$$

where I_{sc} is called as the photo current and it is a function of the solar irradiance on the surface of the solar cell (G) and the cell temperature (T_c). I_{scR} is the short circuit current at the reference solar radiation (G_R) and the reference cell temperature (T_{cR}). The G_R and T_{cR} are called as the Standard Test Conditions (STC). The parameter α_T is the temperature coefficient of photo current generated by the solar cell. The current I_c in Eq. (7) is called as dark current, a function of cell temperature alone. I_{cR} is the dark current at the reference temperature. All of the constants in the Eqs. (5)–(8) can be obtained by examining the manufacturer's catalogue of the PV. A PV array is modelled as series and parallel-connected modules and the single cell circuit can be scaled up to represent any series/parallel combination. The output obtained from the PV system is fed to the inverter system which is connected to the microgrid through the circuit breaker.

2.4. Modelling of PEM fuel cell system

The fuel cell is the energy conversion device which generates electrical energy from the chemical energy. The Avista labs SR-12 500 W PEM fuel cell stack is modelled as a separate DG and the modelling is done using PSCAD based on [12]. In this work, the activation loss, ohmic loss and concentration loss are included in the proposed PEM fuel cell stack. The anode pressure (PA), cathode pressure (PC), fuel cell initial temperature (TI) and room temperature (TR) are the inputs and fuel cell voltage (VFC) is the output of the proposed PEM fuel cell model. The current from the fuel cell (IFC) determines the internal temperature (T). The T and IFC are taken as feedback which is also used to calculate the VFC. Therefore, the average voltage of the fuel cell is given as,

$$V_{cell} = E_{nernst} - V_d - IR \tag{9}$$

2.5. Modelling of battery energy storage system

The Battery Energy Storage System (BESS) using PSCAD is modelled based on the controlled DC voltage source [13–15]. The source can be modelled as battery because the output of the source is controlled with fixed power and voltage. The most important characteristics of a battery are determined by the voltage of their cells, the current capable of supplying over a given time (measured in A h), the time constants and its internal resistance. The two electrodes that supply or receive power are called positive electrodes (*ep*) and negative (*en*), respectively. Inside the battery, the ions are transported between the negative and positive electrodes through an electrolyte. The electrolyte is liquid. The electromotive force E_0 is the voltage difference between the electrode potentials for an open external circuit or at no load, defined as follows:

$$E_0 = E_{ep} - E_{en} \tag{10}$$

The BESS is modelled with the charging system, which is charged for the grid on the basics of program based on State of Charge (SOC). Most SOC methods take into account voltage and current as well as temperature and other aspects of the discharge and charge process to in essence count up or down within a pre-defined capacity of a BESS. The drawback of the model is that, in the modelled BESS the SOC is resolute only based on voltage. Therefore, the terminal voltage of a BESS stays significantly constant until it is completely discharged.

3. Development of adaptive protection scheme for microgrid

The protection scheme is developed individually for the grid connected mode of operation and islanded mode of operation. Finally, these schemes are integrated into a single protection scheme by employing adaptive selection of operation. This adaptive nature of the protection scheme will change the protection relay setting depending upon the modes of operations. Moreover, the proposed protection strategy also uses Microgrid Communication Medium (MCM) to communicate with all relays and DGs in the microgrid. The MCM updates the operating currents of the relays, detects the fault current and signals the CB to trip instantaneously.

3.1. Protection strategy for the grid connected mode of operation

The flow chart for grid connected protection scheme is shown in Fig. 3(a). In grid connected mode, the proposed protection algorithm makes the continuous measurement of voltage and current of ach bus and the feeders and sends them to MCM. When the fault occurs in the microgrid during grid connected mode, the MCM detects the fault by means of negative sequence component and initiates the protection algorithm. Furthermore, on detecting the fault, the MCM determines

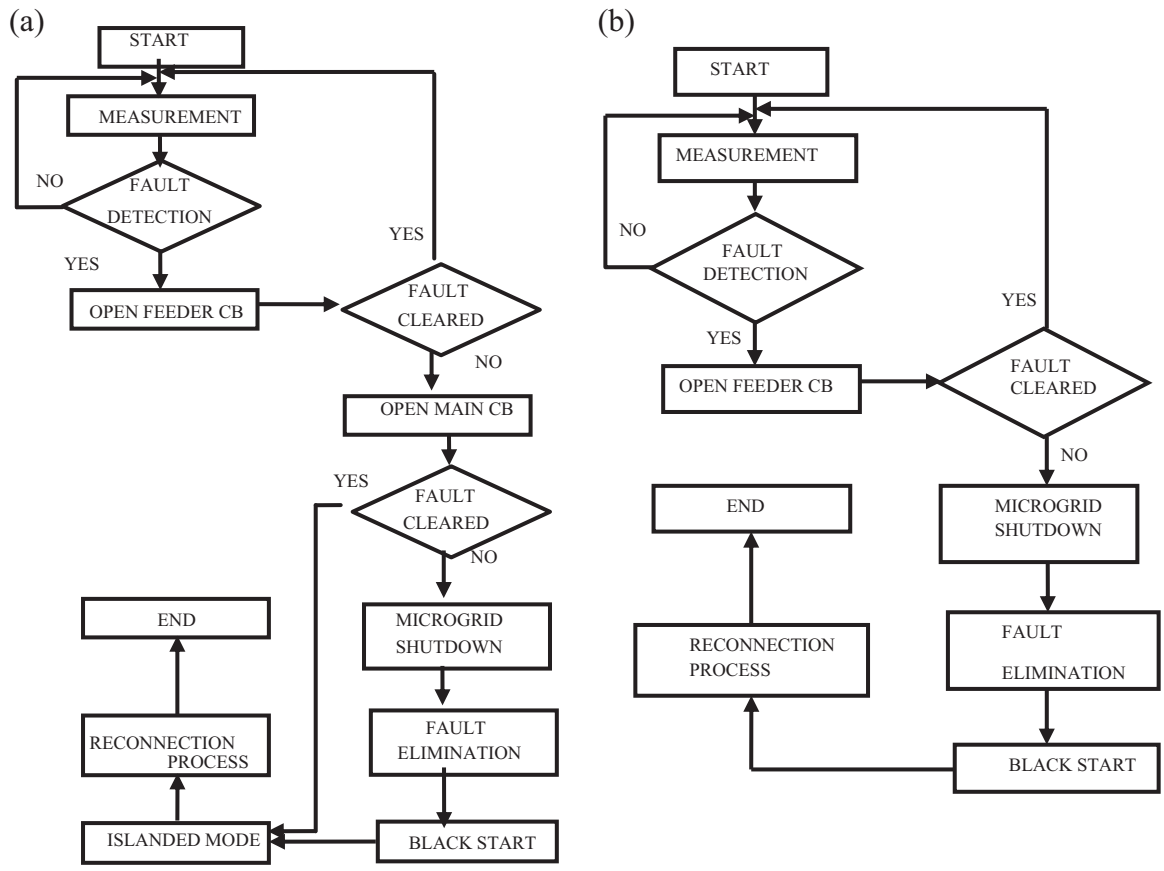

Figure 3 (a) Protection scheme in grid connected mode, (b) protection scheme in islanded mode of operation.

the tripping time for the relay, using the inverse definite time and over-current relay component of the adaptive protection scheme. Firstly, the MCM gives the trip command to the respective Circuit Breaker (CB) of the feeder. If the occurred fault is examined to have positive sequence current, the MCM commands the protection algorithm to reset. Further, MCM continues the monitoring. In case if negative sequence current is found, the MCM communicates with the particular feeder to trip from the microgrid and fault clearance is carried out. Again the MCM checks whether the fault gets eliminated or not. If the fault gets cleared the MCM commands the protection algorithm to reset and continues the monitoring. Else, the trip command from the MCM is given to the main CB and fault clearance is carried out. Again the MCM checks whether the fault gets eliminated or not after a definite time period. If the fault is cleared the MCM switches the microgrid to enter the islanding mode and starts its reconnection process to its normal grid connected operation. The MCM identifies the system frequency and voltage to decide whether to shut down the microgrid or not, if the fault does not get cleared. With the abnormal frequency and voltage, the MCM sends signal to shut down the microgrid and the fault is eliminated physically. Further, the microgrid is started from the black start in islanding mode. Then, the microgrid enters the reconnection process to proceed the normal operating state as indicated in the flowchart.

The feeder protection relays are responsible for the individual feeders and the synchronization among the feeders. They are enhanced by the main protection relay installed near the main CB. The main protection relay responds by opening the main CB only when there is defeat in grid and to the grid side disturbances.

3.2. Protection strategy for the islanded mode of operation

In the islanded mode of operation, the MCM makes the continuous measurement of the voltage and the current of the each bus and feeder, respectively. When the instantaneous fault occurs in the system, the MCM initiates the fault detection through the symmetrical components and the dq-component based comparison [17]. The pickup value of relays used in the islanded mode is very much less than that of grid connected mode. On detection of the fault, if the sequence current is positive the MCM commands the protection algorithm to reset and continues the monitoring. In case of negative sequence current, MCM determines the tripping time for the relay, using the inverse definite time and over-current relay component of the adaptive protection relay. Then the MCM gives the trip command to the respective feeder CB and the particular feeder gets tripped from the microgrid and the fault clearance is carried out. The opening of the feeder CB in the islanded mode of operation makes the microgrid unstable. The remaining feeders in the islanded microgrid system cannot able to supply enough requirements to the load. In that case, the MCM shut downs the microgrid until the fault is eliminated manually.

Therefore, after fault clearance the microgrid starts from black start and takes reconnection process as indicated in the flow chart shown in Fig. 3(b).

Thus, the protection scheme for the grid connected mode and the islanded mode is developed separately. An adaptive controller changes the working mode of the relay based on the mode of operation. The adaptive protection scheme is applicable for all types of fault in the microgrid system.

4. Modelling the proposed adaptive protective relay

The proposed protective relay is developed by means of sequential components as shown in Fig. 4. The feeder current and voltages are measured using current transformer and potential transformer. Further, they are transformed into sequential voltage and current components through suitable transformation. The positive sequence component of the feeder current is used to monitor the current flow in the feeder [27]. If any overcurrent flows, it is detected by means of the overcurrent relay which also determines the time of tripping using the Inverse Definite Minimum Time (IDMT) characteristics [28]. Events such as unbalance and single phasing are detected using the negative sequence components of the feeder current and tripping of the CB is done, if the disturbance sustains for a definite time period. The ground faults are detected using the zero sequence components. Similarly, the events such as under voltage and over voltage are detected by means of sequence components of the voltage. On detecting the disturbance in the voltage for a sustained duration, the CB gets tripped using the trip command. Further, the frequency relay monitors the microgrid frequency. When the operating frequency gets deviated beyond the acceptable operating frequency range measured using the Phase Locked Loop (PLL) the main CB gets tripped.

The final trip signal is sent to CB through an Auto Reclosure Module (ARM). The main function of this module is to reclose the CB after definite time period to check whether the trip is due to a temporary fault [29]. If the trip is due to a temporary fault, the microgrid returns to operation when the reclosure is done. If it is permanent fault then ARM keeps CB in open condition till the fault is cleared. In addition to this set-up, a separate single phase disturbance event detection module is used to detect the faults in any of the three phases and the faults which might not have been detected by the main protection module. The proposed protection relay can be practically developed using a microcontroller based system. This type of system offers additional services such as event reporting, data logging, and communication links.

In order to protect the EC-DGs connected to the microgrid during the time of disturbances and faults, the protection relay gives trip command to both feeder CB and EC-DG's CB. The adaptive protection is implemented by monitoring the main CB status and then applies the change of relay setting based upon the mode of operation. Practically, these settings are stored in the memory of the controller. These settings are then retrieved based upon the mode of operation and adaptive protection is enhanced in the microgrid.

To implement the proposed protection strategy, the common communication service MCM is viable for all locations of the microgrid. The advancement in the recent wireless technologies provides standardized practices that may be suitable for the wide area, metropolitan area and local area. This

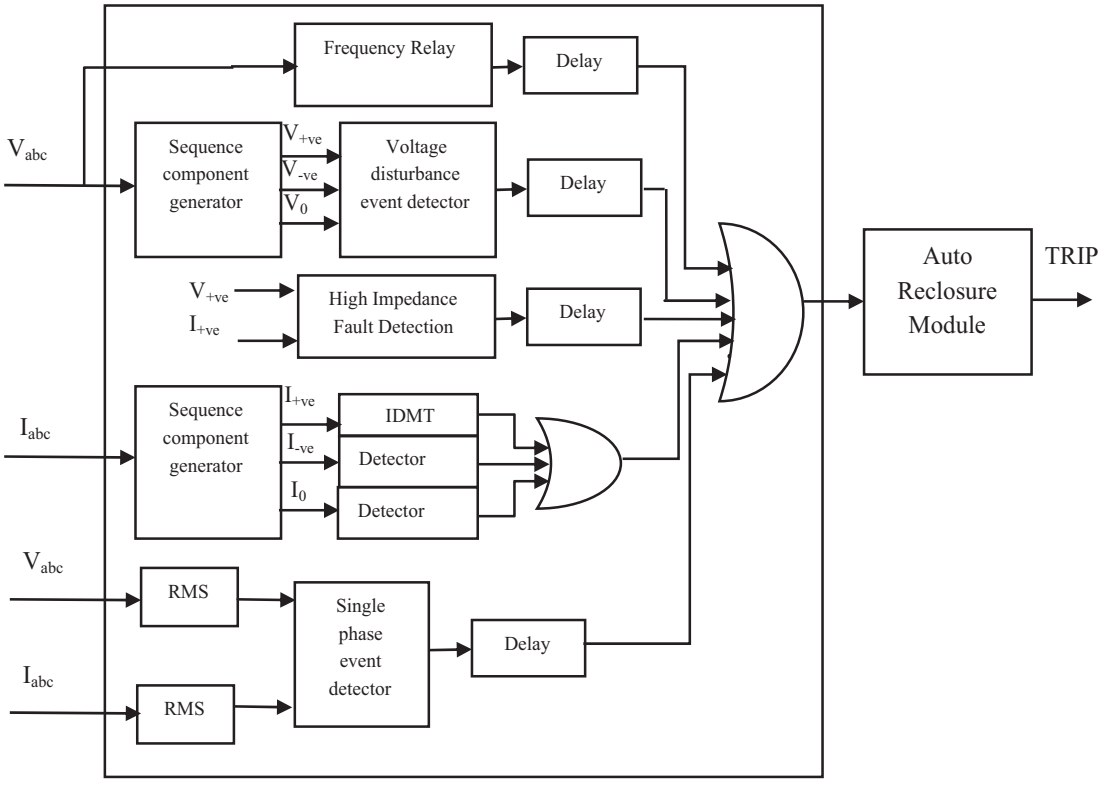

Figure 4 Proposed adaptive protection relay.

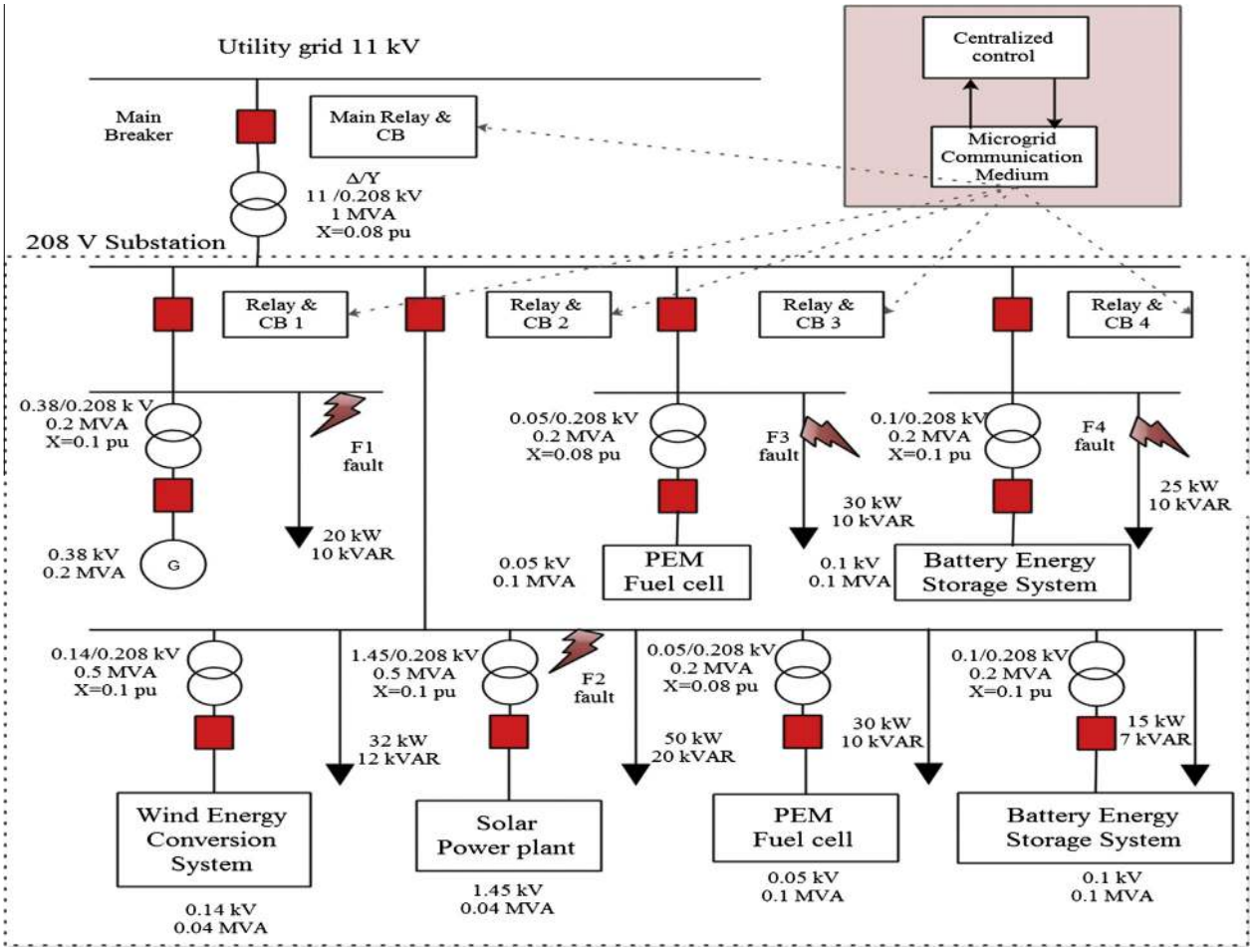

Figure 5 Test system.

Table 1 Over-current relay inverse-time sitting for feeder and main CB.

Parameter	Symbol	Value
Feeder 1 time setting	t_1	0.8
Feeder 2 time setting	t_2	0.8
Feeder 3 time setting	t_3	1.0
Feeder 4 time setting	t_4	0.6
Main CB time setting	t_m	1.2
Inverse pick-up current	I_{inv}	5A

MCM infrastructure enables coordinated protection strategy with protection coordinating module. The wireless communication based MCM possesses many advantages over the wired communication in terms of low installation cost, rapid deployment, increased mobility and covering the remote places.

4.1. Development of the test system

The test system is built using PSCAD (Power Systems CAD) V4.2. The test system is originally adopted from the benchmark of the low voltage microgrid developed by CIGRE (International Council on Large Electric Systems) and the

Table 2 Values of time delay for the main CB and feeder.

Parameter	Symbol	Feeder value (ms)	Main CB value (ms)
Island forward mode delay	t_{d_if}	433	50
Island reverse mode delay	t_{d_ir}	50	433
Grid connected forward mode delay	t_{d_gf}	16.7	5
Grid connected reverse mode delay	t_{d_gr}	50	200
3Φ forward mode delay	t_{d_pf}	566	250
3Φ reverse mode delay	t_{d_pr}	250	633
Instant delay for overcurrent relay	t_{d_oc}	500	500
Low impedance fault delay	t_{d_hir}	500	500

parameters are taken from [30,31]. The test system contains basically a small scale radial network with 208 V, four feeders and DG system. The DG is connected to the test system through an electronic coupler or inverter system and an 11 kV feeder. The test system consists of the Δ/Y step down transformer through which the utility is connected to the microgrid. Each EC-DG is modelled separately and integrated to build the test system. The utility grid is symbolized by an

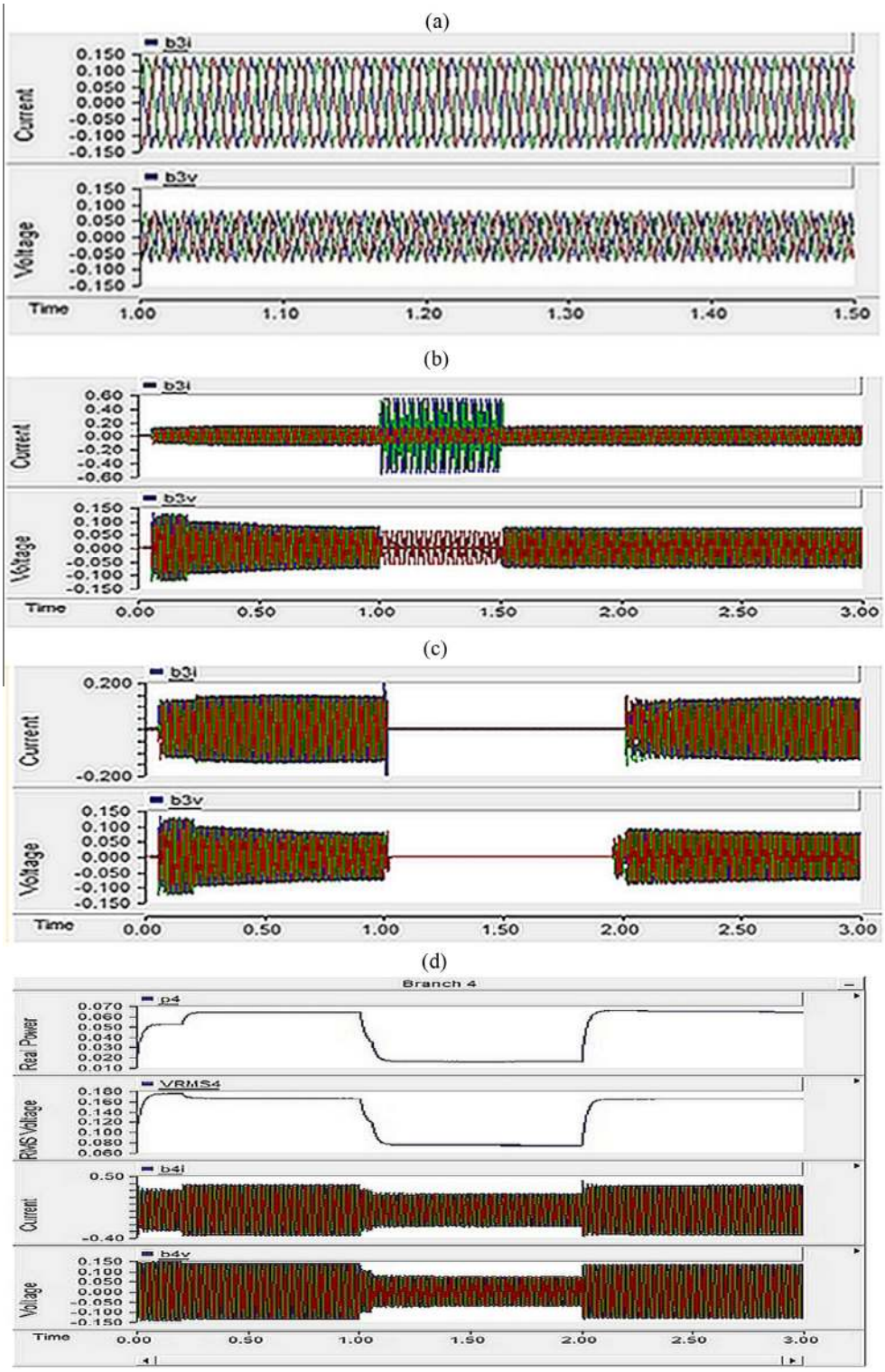

Figure 6 (a) Instantaneous voltage and current in feeder 3, (b) instantaneous voltage and current in feeder 3 with double line to ground fault, (c) instantaneous voltage and current in feeder 3 with double line to ground fault with protection scheme applied, and (d) power flow.

Table 3 Relay operating time for the various faults.

Faults	Low impedance fault	
	Grid connected mode operating time (s)	Islanded mode operating time (s)
F1 fault in feeder 1	0.05	0.06
F2 fault in feeder 3	0.02	0.02
F3 fault in feeder 4	0.02	0.02
F4 fault in feeder 2	0.105	NA

Table 4 Negative sequence values obtained for the network.

Relay no.	Normal operation in grid connected mode (kA)	Faulted condition in grid connected mode (kA)	Normal operation in islanded mode (kA)	Faulted condition in islanded mode (kA)
1	0.003	0.01	0.009	0.0227
2	0.016	0.1	0.056	0.21
3	0.0012	0.0325	0.0035	0.06
4	0.0059	0.066	0.0098	0.08

11 kV bus with a short circuit capacity of 80 MVA. Different combinations of 3Φ and 1Φ loads are connected to the microgrid through the feeders. The test system includes 3Φ EC-DG linked to test system and sub mains, respectively through a Δ/GY interconnected transformer. The DGs used in the system are the wind, solar and battery storage systems. All the EC-DGs are modelled to supply the loads during the grid connected as well as the islanded mode of operation. The complete schematic diagram of the test system is shown in Fig. 5.

The test system uses four feeders and they are named feeder 1, feeder 2, feeder 3 and feeder 4. The feeder 1 is connected with sub mains, i.e., connecting the utility through alternate substation rather than through the substation and through which the 11 kV feeder is connected. The feeder 3 and feeder 4 are exclusively connected to the battery storage system. The feeder 2 is connected with EC-DER such as wind, solar and BESS. Each feeder is provided with a breaker named CB1, CB2, CB3 and CB4. The microgrid can suffer from the faults such as feeder fault, fault in the load, microgrid bus fault and fault in the external grid. These faults are simulated in the microgrid through the faults F1, F2, F3 and F4. The faults F1, F2, F3 and F4 are applied in feeder 1, feeder 2, feeder 3 and feeder 4, respectively. The performance of the protection scheme is studied through the simulation.

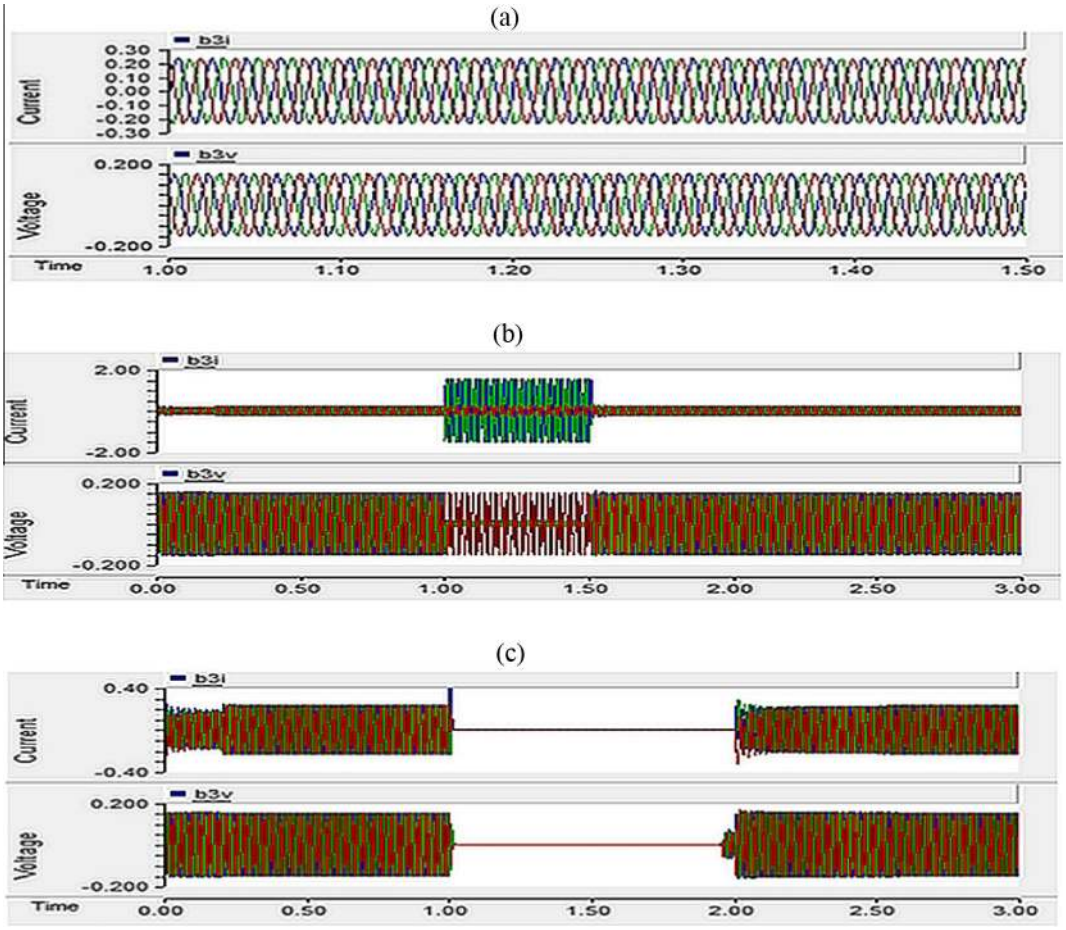

Figure 7 Voltage and current in the feeder 3 after the clearance of the fault (a) instantaneous voltage and current in feeder 3, (b) instantaneous voltage and current in feeder 3 with double line to ground fault, and (c) instantaneous voltage and current in feeder 3 with double line to ground fault with protection scheme applied.

5. Results and discussions

5.1. Simulation results

To illustrate the efficiency of the proposed protection scheme, a low voltage microgrid system has been simulated using PSCAD/EMTDC software environment. The framework of the simulated microgrid is described in Section 4.1 and it is referred to as "test system". In this study, two different cases are considered for analysis, namely islanded mode and grid connected mode of operation.

5.1.1. Islanded mode of operation

The test system is provided with the feeder relay setting and time delay setting with the determined values as listed in Tables 1 and 2. Fig. 6(a) shows the voltage and current obtained during the normal operation of the microgrid. Let us consider an LLG fault between A and B phases of feeder 3 at $t = 1$ s. In the islanded mode of operation, the impact of fault could result in inadequate fault current. However, in case of temporary fault, the proposed protective scheme detects and clears the fault through the ARM system. In case of low impedance fault, it affects the instantaneous voltage and current as shown in Fig. 6(b). It can be observed that the fault current in the islanded mode is 1.85 p.u and 0.6 p.u. Hence, a common protection setting cannot be used to eliminate the fault occurred. Therefore, the proposed protection strategy is implemented; it changes the relay setting automatically according to the type of faults. Further, the protection coordination receives signal from MCM and commands the CB3 to open. The ARM is initiated by MCM in the feeder 3, and it rides through the faults and eliminates them after certain time at

Table 5 Operating time and relays for the faults in both modes of operation.

Protection strategy	Fault loc.	Grid connected mode				Islanded mode			
		Primary protection		Backup protection		Primary protection		Backup protection	
		Opera. relay	Oper. time (s)	Oper. relay	Oper. time (s)	Oper. relay	Oper. time (s)	Oper. relay	Oper. time (s)
Proposed microprocessor based prot. scheme	F1	FEEDER 1	0.058	Main CB	0.50	FEEDER 1	0.063	FEEDER 1	0.273
				FEEDER 1	0.272				
				FEEDER 2	0.625			FEEDER 2	0.65
				FEEDER 3	0.625			FEEDER 3	1.50
				FEEDER 4	0.600			FEEDER 4	0.675
	F2	FEEDER 2	0.105	Main CB	0.700	FEEDER 2	0.028	FEEDER 1	0.675
				FEEDER 1	0.750				
				FEEDER 2	0.274			FEEDER 2	0.273
				FEEDER 3	0.650			FEEDER 3	0.650
				FEEDER 4	0.625			FEEDER 4	0.650
	F3	FEEDER 3	0.026	Main CB	0.611	FEEDER 3	0.027	FEEDER 1	0.675
				FEEDER 1	1.20				
				FEEDER 2	1.20			FEEDER 2	0.650
				FEEDER 3	0.274			FEEDER 3	0.272
				FEEDER 4	0.625			FEEDER 4	0.650
	F4	FEEDER 4	0.028	Main CB	2.00	FEEDER 4	0.028	FEEDER 1	0.675
				FEEDER 1	1.80				
				FEEDER 2	1.50			FEEDER 2	0.650
				FEEDER 3	1.20			FEEDER 3	0.625
				FEEDER 4	≃1.0			FEEDER 4	0.277
Conventional microproces-sor based prot. scheme	F1	FEEDER 1	0.054	Main CB	0.615	FEEDER 1	0.084	FEEDER 1	0.283
				FEEDER 1	0.286				
				FEEDER 2	0.688			FEEDER 2	0.686
				FEEDER 3	0.691			FEEDER 3	≃4.0
				FEEDER 4	0.655			FEEDER 4	0.682
	F2	FEEDER 2	0.031	Main CB	0.619	FEEDER 2	0.086	FEEDER 1	0.685
				FEEDER 1	0.689				
				FEEDER 2	0.288			FEEDER 2	0.285
				FEEDER 3	0.693			FEEDER 3	0.685
				FEEDER 4	0.685			FEEDER 4	0.685
	F3	FEEDER 3	0.189	Main CB	0.611	FEEDER 3	0.082	FEEDER 1	0.685
				FEEDER 1	≃4.0				
				FEEDER 2	≃4.0			FEEDER 2	0.684
				FEEDER 3	0.285			FEEDER 3	0.283
				FEEDER 4	0.682			FEEDER 4	0.684
	F4	FEEDER 4	0.184	Main CB	≃4.0	FEEDER 4	0.080	FEEDER 1	≃4.0
				FEEDER 1	≃4.0				
				FEEDER 2	≃4.0			FEEDER 2	≃4.0
				FEEDER 3	≃4.0			FEEDER 3	≃4.0
				FEEDER 4	≃3.5			FEEDER 4	≃3.5

t = 1.5 s. Fig. 6(c) shows the instantaneous voltage and current obtained after the protection scheme is applied. Fig. 6(d) shows the normal flow of power, voltage and current in feeder 3 after the termination of the faults. In systems with high complexity and large systems, the protection coordination can be enhanced by the evolutionary optimization techniques. The operating time for various faults induced in the system is tabulated in Table 3. It can be observed from Table 3 that any fault in feeder 2 in islanded mode makes the microgrid unstable. The reason for the instability is due to the presence of all EC-DGs in the feeder 2. If any fault opens the CB2 of the feeder 2, the microgrid demand cannot be met using the remaining DG. Hence, the microgrid is fully shutdown. During this crucial time, the fault in the microgrid should be removed manually and the microgrid starts from black start. Thus, sufficient care must be taken to avoid fault in feeder 2 during the islanded mode. The fault detection in feeder as discussed in Section 4 is enhanced through the negative sequence component. The negative sequence values obtained from grid connected mode and islanded mode are used for the detection of fault and are listed in Table 4.

5.1.2. Grid connected mode of operation

Several studies are carried out on the test system and the system is provided with relay settings and delay time settings as discussed in Tables 1 and 2. During normal operation of the microgrid, there exerts efficient coupling with the utility. Fig. 7(a) shows the instantaneous voltage and current in feeder 3 during normal operation of the microgrid. Let us consider an LLG fault between A and B phases of feeder 3 at t = 1 s and prolongs for more than one sec. Based on the severity of the fault occurred, the time of tripping is determined by MCM and commands are send to the overcurrent relay. From Fig. 7(b) it can be observed that a double phase to ground fault in phases A and B of feeder 3 prolongs from 1 to 1.5 s. Protection scheme protects the feeder as shown in Fig. 7(c), and the same process is followed as discussed in island mode of operation. In some occasion, if the external fault occurs in the test system, the negative sequence relay senses the indication of the commencement of the fault and the fault is processed by the overcurrent relay. For the temporary faults, the reclosure ARM module recloses after 0.015 s after riding the temporary fault and provides a reliable grid protection. If the fault prolongs, the protective scheme opens the breaker CB3 and the main-breaker of DG system is connected to that feeder after 0.02 s. Further, the time of tripping is determined MCM for the overcurrent relay and the operating timings of the relays for various faults are listed in Table 3.

Table 5 shows the operating time of feeders in both grid connected mode and islanded mode for primary protection and backup protection. In case of temporary fault, it can be observed that the proposed methodology rides through the faults and return backs the normal operation as quick and reliable when compared to conventional method. Further, during low impedance protection it can be observed that proposed methodology works reliable and effectively.

5.2. Comparative analysis

In order, to analyse the effectiveness of the proposed protection scheme on the developed test system, a comparative study is carried out between the proposed protection scheme and conventional protection scheme. The operating time obtained for primary protection and backup protection of low impedance fault in grid connected and islanded mode is listed in Table 5.

It is observed that the operating time of the feeders is reduced in both grid connected mode and islanded mode for primary protection and backup protection, compared to the conventional microprocessor relay modification. In case of temporary fault, it can be observed that the proposed methodology rides through the faults and returns back quickly to the normal operation and it is reliable, compared to the conventional method. During low impedance protection, it can be observed that the proposed methodology works reliably than the conventional technique by enhancing the faster operation of the feeder relays. As a result, this proposed protective scheme can be viable for all kinds of faults in the microgid.

6. Conclusion

The main objective of this paper was to address some concerns related to the protection of microgrids. The problems studied in this paper are (i) modelling EC-DERs to form microgrid, and (ii) protection of the microgrid against different fault conditions in both modes of operation. The DGs such as solar, fuel cell, BESS and wind are modelled and integrated to the microgrid using the developed converter system. The adaptive protection strategy is implemented using the proposed methodology. The relay is modified for overall protection of the microgrid. Further, the proposed protection scheme rides through any temporary faults and returns quickly to the pre-faulted conditions. Further, during low impedance fault they act so reliable and quicker. Hence, the proposed protective relay performs adequately and provides suitable protection in both grid-connected and islanded modes of operation. Moreover, the simulation results demonstrate the success of the developed adaptive protection scheme of the microgrid.

Acknowledgement

The authors are thankful to the authorities of Thiagarajar College of Engineering, Madurai-625015, India and MVJ College of Engineering, Banglore-67, India, for providing all the facilities to do the research work.

References

[1] C. Smallwood, Distributed generation in autonomous and non-autonomous microgrids, in: IEEE 2002 RUR ELEC P, Colorado Springs, 2002, pp. 1–6.
[2] R.H. Lasseter, Microgrids, in: IEEE 2002 Power Eng Soc, 2002, pp. 305–308.
[3] N. Hadjsaid, J.F. Canard, F. Dumas, Dispersed generation impact on distribution networks, IEEE Trans. Comput. Appl. Power 12 (1999) 22–28.
[4] S. Chowdhury, P. Crossley, Microgrids and Active Distribution Networks, The Institution of Engineering and Technology, 2009.
[5] A. Girgis, S. Brahma, Effect of distributed generation on protective device coordination in distribution system, in: IEEE Large Engineering Systems Conference, 2001, pp. 115–119.
[6] H. Wan, K.K. Li, K.P. Wong, An multi-agent approach to protection relay coordination with distributed generators in

industrial power distribution system, in: IEEE Ind Applic Soc, 2005, pp. 830–836.
[7] S.M. Brahma, A. Girgis, Development of adaptive protection scheme for distribution systems with high penetration of distributed generation, IEEE Trans. Power Delivery 19 (2004) 56–63.
[8] P. Basak, S. Chowdhury, S. Halder, S.P. Chowdhury, A literature review on integration of distributed energy resources in the perspective of control, protection and stability of microgrid, Renew. Sustain. Energy Rev. 16 (2012) 5545–5556.
[9] N. Schäfer, T. Degner, A. Shustov, T. Keil, T. Jäger, Adaptive protection system for distribution networks with distributed energy resources, in: IET Developments in Power System Protection, 2010, pp. 1–5.
[10] S. Conti, L. Raffa, U. Vagliasindi, Innovative solutions for protection schemes in autonomous MV micro-grids, in: IEEE International Conference on Clean Electrical Power, 2009, pp. 647–654.
[11] E. Sortomme, J. Mitra, S.S. Venkata, Microgrid protection using communication assisted relays, IEEE Trans. Power Delivery 25 (2010) 2789–2796.
[12] M. Park, D.H. Lee, I.K. Yu, PSCAD/EMTDC modeling and simulation of solar-powered hydrogen production system, Renewable Energy 31 (2006) 2342–2355.
[13] S. Koohi-Kamal, N.A. Rahim, H. Mokhlis, Smart power management algorithm in microgrid consisting of photovoltaic, diesel, and battery storage plants considering variations in sunlight, temperature, and load, Energy Convers. Manage. 84 (2014) 562–582.
[14] M.A. Zamani, T.S. Sidhu, A. Yazdani, A communication-based strategy for protection of microgrids with looped configuration, Electr. Power Syst. Res. 104 (2013) 52–61.
[15] M. Mazidi, A. Zakariazadeh, S. Jadid, S. Siano, Integrated scheduling of renewable generation and demand response programs in a microgrid, Energy Convers. Manage. 86 (2014) 1118–1127.
[16] H.J. Laaksonen, Protection principles for future microgrids, IEEE Trans. Power Electron. 25 (2010) 2910–2918.
[17] M.A. Zamani, T.S. Sidhu, A. Yazdani, A protection strategy and microprocessor-based relay for low-voltage microgrids, IEEE Trans. Power Delivery 26 (2011) 1873–1883.
[18] M.H. Moradi, M. Eskandari, H. Showkati, Hybrid method for simultaneous optimization of DG capacity and operational strategy in microgrids utilizing renewable energy resources, Int. J. Electr. Power 56 (2014) 241–258.
[19] T.S. Ustun, R.H. Khan, A. Hadbah, A. Kalam, An adaptive microgrid protection scheme based on a wide-area smart grid communications network, in: IEEE Latin-America Conference on Communication, 2013, pp. 1–5.
[20] H. Al-Nasseri, M.A. Redfern, F. Li, A voltage based protection for micro-grids containing power electronic converters, in: IEEE Power Engineering Society General Meeting, 2006, pp. 7–12.
[21] T. Loix, T. Wijnhoven, G. Deconinck, Protection of microgrids with a high penetration of inverter-coupled energy sources, in: IEEE Integration of Wide-Scale Renewable Resources into the Power Delivery System, PES Joint Symposium, 2009, pp. 1–6.
[22] P. Vas, Sensorless Vector and Direct Torque Control, Oxford Science Publications, New York, 1998.
[23] S. Heier, Grid Integration of Wind Energy Conversion Systems, John Wiley & Sons, Germany, 2006.
[24] T. Ackermann, Wind power in power systems, John Wiley, Chichester, UK, 2005.
[25] R. Sitharthan, M. Geethanjali, An adaptive Elman neural network with C-PSO learning algorithm based pitch angle controller for DFIG based WECS, J. Vib. Control (2015), http://dx.doi.org/10.1177/1077546315585038.
[26] E. Villanueva, P. Correa, J. Rodríguez, M. Pacas, Control of a single-phase cascaded H-bridge multilevel inverter for grid-connected photovoltaic systems, IEEE Trans. Ind. Electron. 56 (2009) 4399–4406.
[27] J.D. Park, J. Candelaria, Fault detection and isolation in low-voltage DC-bus microgrid system, IEEE Trans. Power Delivery 28 (2013) 779–787.
[28] M.B. Delghavi, A. Yazdani, A control strategy for islanded operation of a distributed resource (DR) unit, in: IEEE Power Eng Soc, 2009, pp. 1–8.
[29] M.R. Islam, A.G. Hossam, Study of micro grid safety & protection strategies with control system infrastructures, Smart Grid Renewable Energy 3 (2012) 1–9.
[30] K. Strunz, R.H. Fletcher, R. Campbell, F. Gao, Developing benchmark models for low-voltage distribution feeders, in: IEEE Power Energy Soc, Gen, Meeting, 2009, pp. 1–3.
[31] S. Papathanassiou, N. Hatziargyriou, K. Strunz, A benchmark low voltage microgrid network, in: CIGRE Symposium, 2005, pp. 1–8.